JP0150091

3.3 Study on the effect of subcooling on vapor film collapse on high temperature particle surface

Yutaka ABE, Daisuke TOCHIO and Hiroshi YANAGIDA

Department of Mechanical Systems Engineering, Yamagata University,
Jonan, Yonezawa, Yamagata, 992-8510
Tel & Fax: 0238-26-3221

E-mail: yutaka@mabeken3.yz.yamagata-u.ac.jp

Abstract

Thermal detonation model is proposed to describe vapor explosion. According to this model, vapor film on pre-mixed high temperature droplet surface is needed to be collapsed for the trigger of the vapor explosion. It is pointed out that the vapor film collapse behavior is significantly affected by the subcooling of low temperature liquid. However, the effect of subcooling on micro-mechanism of vapor film collapse behavior is not experimentally well identified. The objective of the present research is to experimentally investigate the effect of subcooling on micro-mechanism of film boiling collapse behavior.

As the results, it is experimentally clarified that the vapor film collapse behavior in low subcool condition is qualitatively different from the vapor film collapse behavior in high subcooling condition. In case of vapor film collapse by pressure pulse, homogeneous vapor generation occurred all over the surface of steel particle in low subcooling condition. On the other hand, heterogeneous vapor generation was observed for higher subcooling condition. In case of vapor film collapse spontaneously, fluctuation of the gas-liquid interface after quenching propagated from bottom to top of the steel particle heterogeneously in low subcooling condition, On the other hand, simultaneous vapor generation occurred for higher subcooling condition.

And the time transient of pressure, particle surface temperature, water temperature and visual information were simultaneously measured in the vapor film collapse experiment by external pressure pulse. Film thickness was estimated by visual data processing technique with the pictures taken by the high-speed video camera. Temperature and heat flux at the vapor-liquid interface were estimated by solving the heat conduction equation with the measured pressure, liquid temperature and vapor film thickness as boundary conditions. Movement of the vapor-liquid interface were estimated with the PIV technique with the visual observation data.

1. Introduction

In the past, large-scale accidents by vapor explosion were occurred in various industrial fields. Thermal detonation model[1] is proposed to describe vapor explosion as shown in Figure 1. The thermal detonation model divides the vapor explosion phenomena into four processes, break-up, pre-mixing, trigger and occurrence of the large-scale vapor explosion. According to the model, vapor film collapse on the pre-mixed high temperature droplet surface is needed to trigger the vapor explosion. In the previous study, it is clarified that the vapor explosion is significantly affected by the subcooling of the low temperature liquid. However, it is not clear how subcooling of the low temperature liquid affect the trigger of the vapor explosion.

Especially, the effect of the subcooling on the micro-mechanism of the vapor film collapse behavior is not well experimentally identified[2], [3], [4]. It is necessary to obtain the experimental information of the micro-mechanism of the vapor film on the high temperature particle surface excluding atmization. The objective of the present research is to experimentally investigate the micro-mechanism of vapor film collapse behavior on the high temperature particle surface.

2. Experiment

2.1 Experimental apparatus

Figure 2 shows the schematic diagram of the experimental apparatus. Test section is composed of the stainless steel square vessel. Its inner dimension is 54 mm, thickness is 3 mm, and length is 316 mm. Polycarbonate plates for the visual observation are installed on three sides of the test vessel. Strain-gauge type pressure transducers are installed on the center of a rest side in order to measure the pressure and to obtain the trigger signal for high-speed video camera. The sheathed thermocouple to measure the water temperature is the test vessel 30 mm above the center. The pressure pulse generator is located at the bottom of the test vessel. The pressure pulse is generated by hitting the piston with a bullet driven by nitrogen gas. The nitrogen gas flow is operated with electromagnetic valve to obtain good repeatability.

Experimental data are recorded as voltage data into analyzing recorder through amplifier. Those data are transferred to the computer through GP-IB. Visual data are obtained by the high-speed video camera of the maximum speed 40,500 fps. The high-speed video camera starts with trigger signal from the pressure transducer
through analyzing recorder.

The detail structure of the stainless steel ball used in the experiment is shown in Fig. 3. The stainless steel ball of 15 mm diameter is suspended with sheathed thermocouple at the center of the test section. The surface temperature of steel ball is measured by the sheathed thermocouple. The thermocouple is inserted into the ball through a hole drilled with electric discharge processing method. The thermocouple is fixed with wedging in the top of the steel ball. The top of the thermocouple is shaved to be naked at the bottom of the steel ball in order to obtain fast temperature response.

2.2 Experimental procedure

Figure 4 shows the experimental procedure. At first, steel ball was heated up to the specified temperature by a burner. Next, the steel ball was submerged into the water to generate the film boiling on the high temperature ball surface. Finally, pressure pulse was generated at the bottom of the test vessel to attack the film boiling on the high temperature ball surface. The vapor film collapse behavior is observed with high-speed video camera.

From the present experimental procedure, the forced vapor film collapse behavior with external pressure pulse is investigated

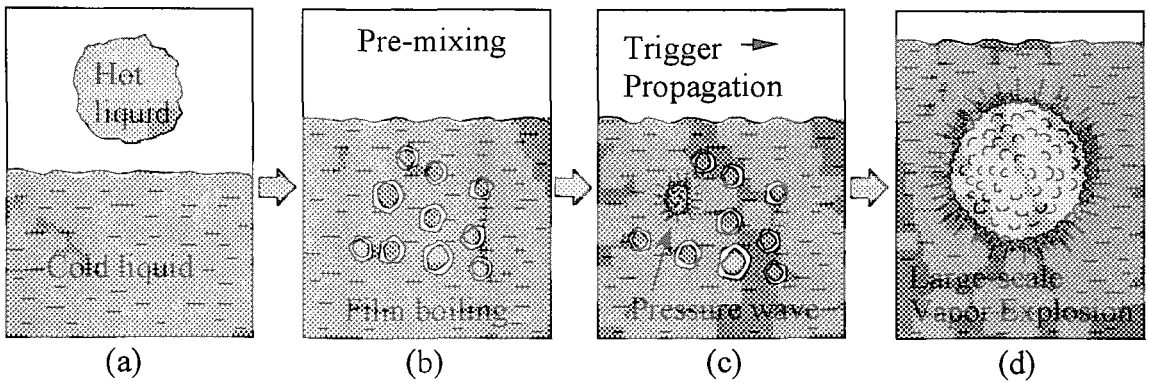

Fig. 1 Thermal detonation model[1]

2.3 Visual data analysis

The graphic data are captured by using the high-speed video camera (Photoron Ltd. FASTCAM-Ultima). Maximum recording speed of the video camera is 40,500 fps for the frame of 64 pixels by 64 pixels and 4,500 fps for the frame of 256 pixels by 256 pixels. The graphic data are stored in the memory unit as 8-bits digital data. The digital data are transferred to a computer through GP-IB interface and stored in MO-drive. The stored digital graphic data are processed to estimate vapor film thickness on the steel particle surface by using the graphical image data processing software. The schematic diagram of the determination procedure of vapor film thickness is shown in Fig.5. The procedure is follows:

1. Capture graphic data of steel particle without vapor film before experiment.
2. Capture graphic data of vapor film collapse on steel particle.
3. Change the 8-bits digital graphic data into binary information. Turn over the binary information of the graphic data with vapor film.
4. Superimpose two graphic binary data.
5. Count the number of pixels of vapor film.

Divide the number of pixels of vapor film by the length of the particle outer surface to estimate the vapor film thickness. The minimum spatial resolution is estimated as 0.02 mm.

3. Results

Figure 6 show the experimental results of pressure and surface temperature. Horizontal axis shows time in ms. It was observed that surface temperature started to decrease when the pressure pulse was arrived.

Symbols of A to F correspond to the pictures below. These pictures were recorded with 4,500 fps. A clear and smooth vapor film was observed at time A before pressure pulse arrived. The peak of the pressure pulse was arrived at time B. At this time, vapor film surface changed white. After the pressure pulse passed away, vapor generation occurred homogeneously all over the surface of the steel particle as shown in C through F.

Figure 7 shows the visual observation results in forced collapse experiment for different subcooling condition. These pictures were recorded with 4,500 fps for subcooling temperature of 8 °C, 18 °C and 25 °C, respectively. In this figure, the arrival time of pressure peak is taken as 0 ms.

Before the arrival of the pressure pulse, clear and smooth vapor film was observed in every condition. The vapor film surface changed white at

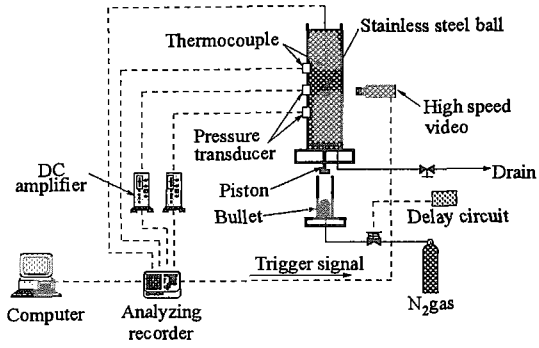

Fig. 2 Experimental apparatus

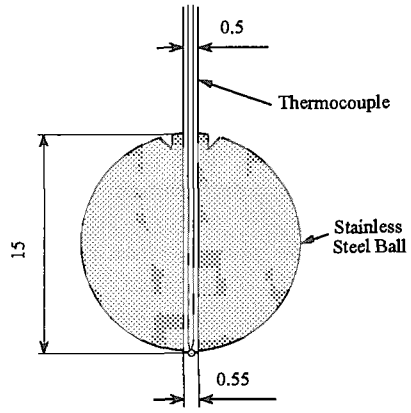

Fig.3 Structure of steel ball

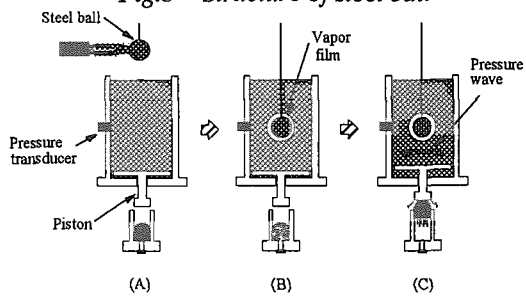

Fig. 4 Experimental procedure

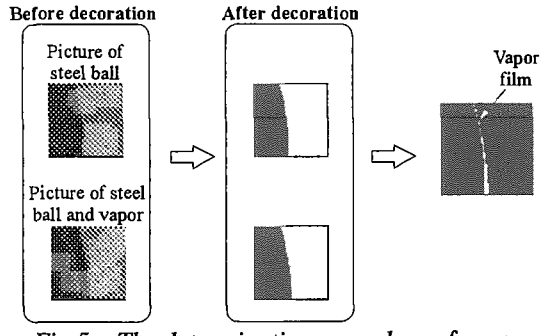

Fig.5 The determination procedure of vapor film thickness

time 0 ms in every condition. It was observed that after the time of pressure pulse passing, homogeneous vapor generation was occurred all over the surface of steel particle in low subcooling condition. On the other hand, the heterogeneous

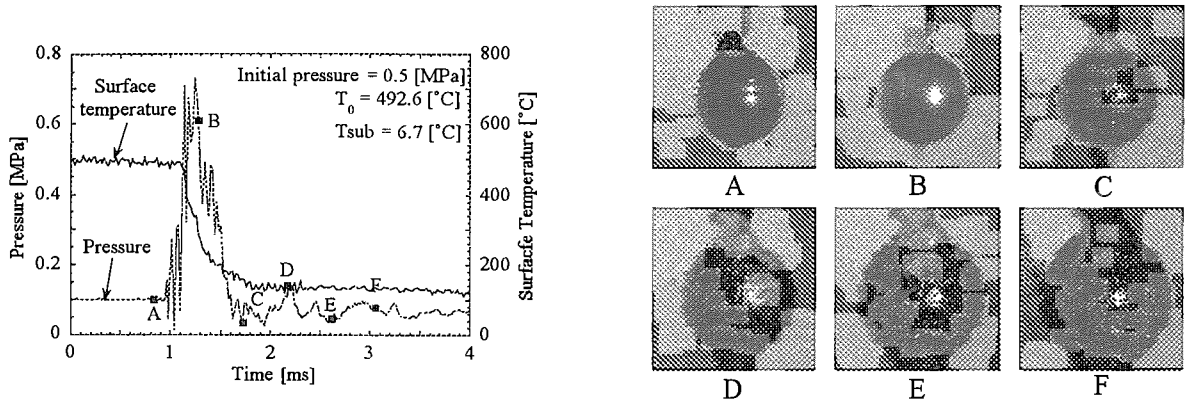

Fig.6 Surface temperature and pressure in forced collapse experiment

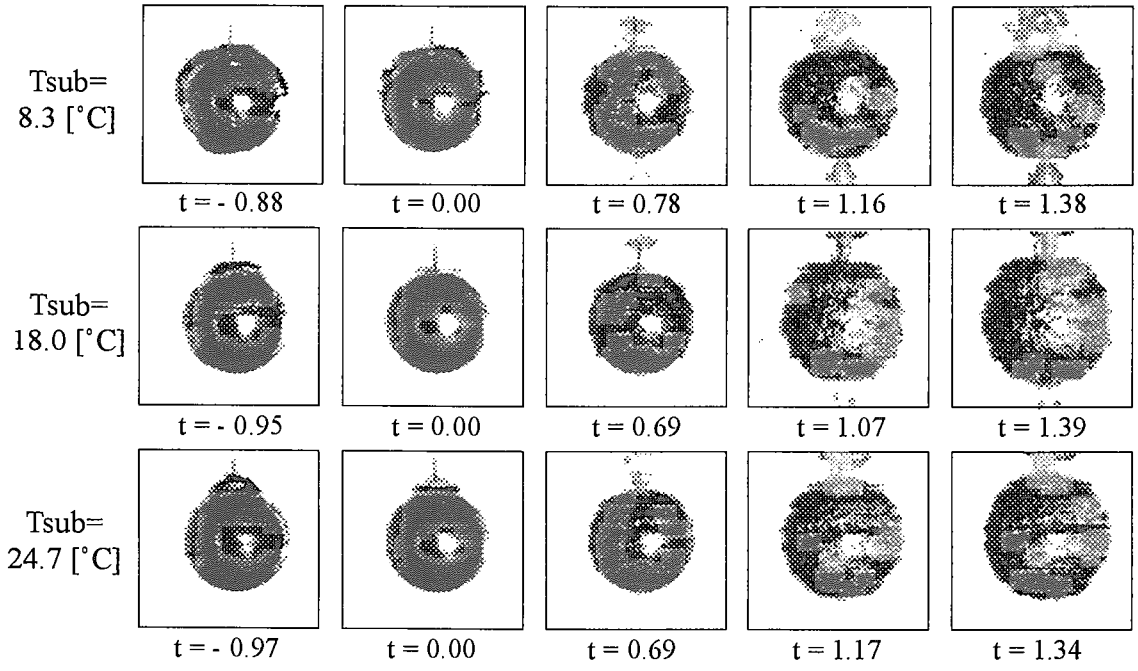

Fig.7 Observation results in forced collapse experiment (unit: ms)

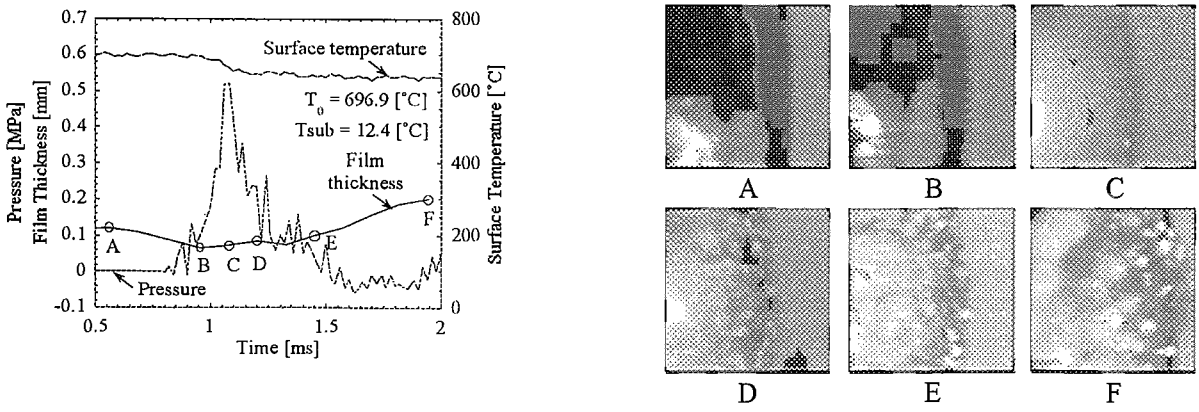

Fig.8 Surface temperature, pressure and film thickness in forced collapse experiment (Tsub=12.4°C).

vapor generation was occurred in high subcooling condition.

Figure 8 show the experimental results of pressure, surface temperature and estimated vapor film thickness. The horizontal axis shows time in ms. Vapor film thickness was estimated from the

visual observation results.

It was observed that surface temperature started decreasing when pressure pulse was arrived. At the time, vapor film thickness decreased to its minimum value. After the estimated vapor film thickness increased quickly.

Symbols of A to F correspond to the pictures below. These pictures were recorded with 40,500 fps. A clear and smooth vapor film was observed before pressure pulse arrived at time A. At time B, vapor film surface changed white as soon as the peak of the pressure pulse was arrived. After the pressure pulse passed away, violent vapor generation occurred as shown in C through F in Fig. 8.

Figure 9 shows the estimated time transient of the vapor film thickness on the steel particle surface for the different subcooling. Symbols of circle, triangle and rectangular show the vapor film thickness for subcooling temperature of 12 °C, 19 °C, and 27 °C, respectively. In Fig. 9, 0 ms is the arrival time of pressure peak.

Before the arrival of pressure pulse, the vapor film thickness for high subcooling condition is lower than that in low subcooling condition. After the arrival of pressure pulse, the vapor film thickness was increased quickly for every subcool condition after the vapor film thickness kept its minimum value for a few milliseconds.

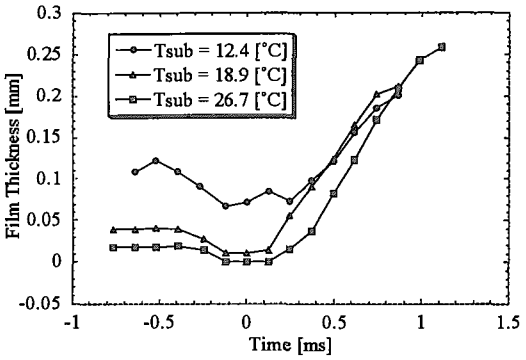

Fig.9 Time variation of film thickness in forced collapse experiment

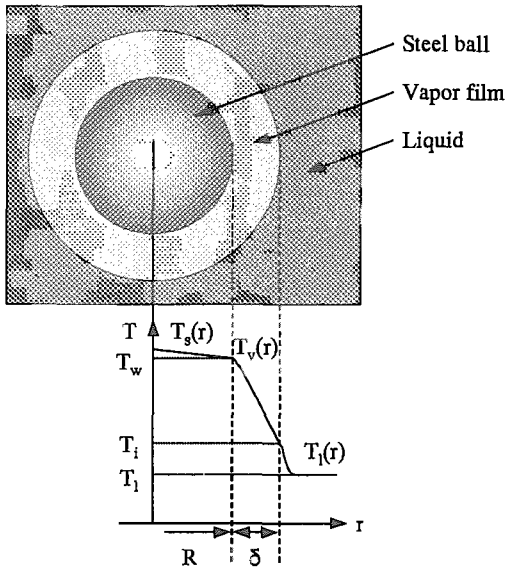

Fig. 10 Schematics of heat conduction analysis

4. Discussion

4.1. Heat conduction analysis

(1) Configuration and procedure of analysis

In order to estimate the vapor-liquid interface, following heat conduction equation is numerically solved.

$$\frac{\partial T}{\partial t} = \kappa \frac{1}{r^2}\frac{\partial}{\partial r}\left(r^2 \frac{\partial T}{\partial r}\right), \qquad (1)$$

where r is distance from the center of the particle, t is time, κ is thermal diffusivity and T is temperature distribution defined as:

$$T(r) = \begin{cases} T_s(r) & (0 < r < R) \\ T_v(r) & (R < r < R + \delta), \\ T_l(r) & (R + \delta < r) \end{cases} \qquad (2)$$

where $T_s(r)$ is the temperature distribution in steel particle, $T_v(r)$ is the temperature distribution in vapor film and $T_l(r)$ is the temperature distribution in liquid. The schematic diagram of the present analysis system is shown in Fig. 10. The system consists of steel particle, vapor film and liquid phase. Complete spherical geometry and homogeneous material properties are assumed in the present analysis. The schematic temperature distribution is also shown in Fig. 10. In the present study, the particle surface temperature T_w, bulk liquid

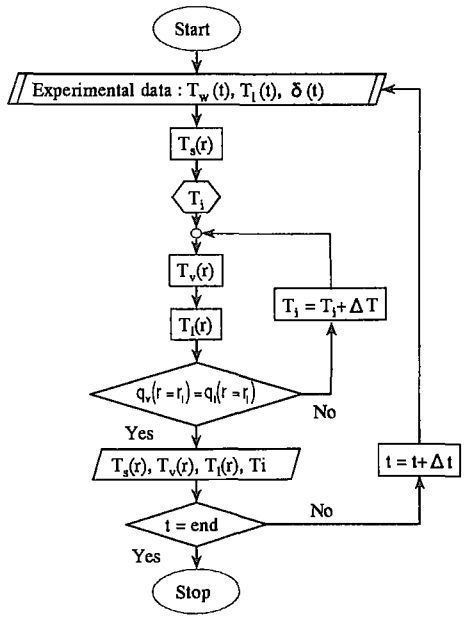

Fig. 11 Flowchart of heat conduction analysis

temperature T_l and vapor film thickness δ were experimentally obtained. Those three data of T_w, T_l and δ were used as boundary conditions to solve the heat conduction equation. The numerical calculation procedure of the heat conduction equation (1) is shown in Fig. 11 as a flow chart. Once the temperature distributions are obtained, the vapor-liquid interface temperature and heat flux can be estimated.

The detail of the solution procedure is as follows:

1. Time transient data of particle surface temperature T_w, liquid temperature T_l and vapor film thickness δ are input as boundary conditions.
2. The temperature distribution in steel particle $T_s(r)$ is calculated.
3. The provisional vapor-liquid interfacial temperature T_i is assumed.
4. The temperature distributions in vapor film $T_v(r)$ and in liquid $T_l(r)$ are calculated.
5. Judged to the heat flux in vapor film is equal to the heat flux in liquid at the vapor–liquid interface.
6. If heat conduction is discontinuous, vapor-liquid interfacal temperature is changed. And the temperature distributions in vapor film and in liquid are calculated again.
7. The procedure 3 through 6 are repeated until the condition of vapor- liquid interfacial heat flux is satisfied.
8. If the condition is satisfied, time step is advanced.

(2) Results of the heat conduction analysis

Figure 12 shows the temperature distribution in steel particle, vapor film and liquid phase. In Fig. 12, the allow lines show the positions of the particle surface and the vapor-liquid interface for different time. The arrival time of pressure peak is taken as 0 ms.

The particle surface temperature was input data obtained from the present experiment. The vapor-liquid interface temperature was not influenced by the change of the particle surface temperature during this short transient period in the present heat conduction calculation.

Figure 13 shows time transient of heat flux at steel particle surface and at vapor-liquid interface. The upper of Fig. 13 shows the time transient of heat flux at particle surface and the lower of Fig. 13 shows that of the vapor-liquid interface. In Fig. 13, the arrival time of pressure peak is as 0 ms.

Heat flux at vapor-liquid interface was estimated three order smaller than that at particle surface. Heat flux was increased quickly at both

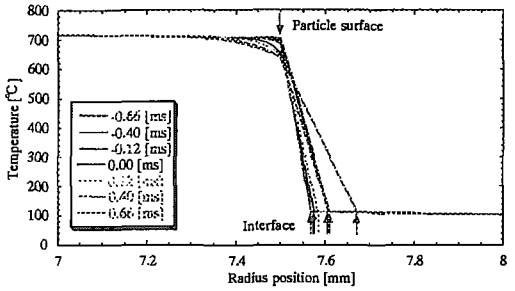

Fig. 12 Temperature distribution in steel particle, vapor film and liquid

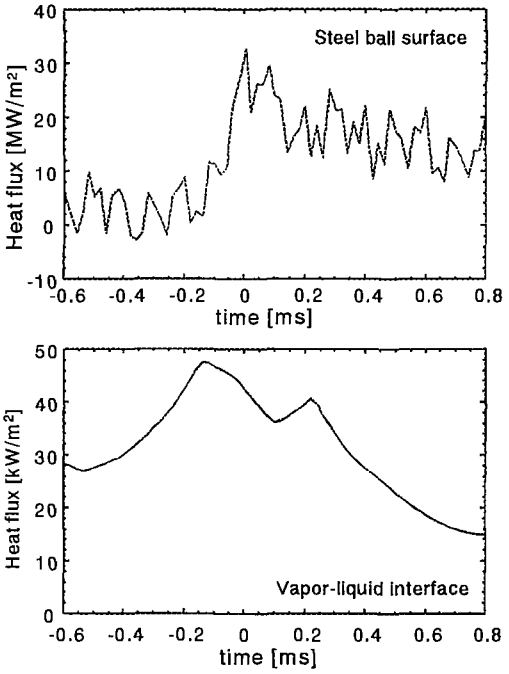

Fig. 13 Time transient of heat flux

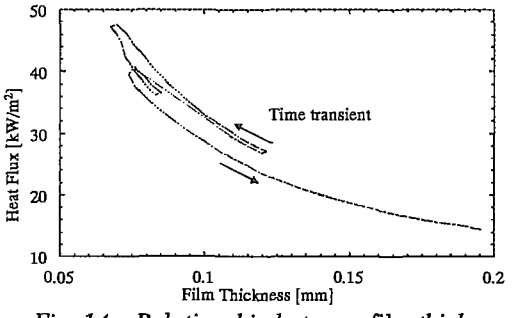

Fig. 14 Relationship between film thickness and heat flux at vapor-liquid interface

sites as soon as the pressure peak arriving. The maximum value of heat flux at particle surface was much higher than that of critical heat flux in pool boiling. Heat flux was gradually decreased at both sites after pressure pulse was passed.

Figure 14 shows relationship between heat flux at vapor-liquid interface and estimated vapor

film thickness. Vertical axis shows heat flux at vapor-liquid interface, horizontal axis shows vapor film thickness. In Fig. 14, allow lines show the time merching. At first, heat flux increased with decreasing vapor film thickness. Then, heat flux decreased with increasing vapor film thickness. In the present heat conduction calculation, heat flux at the vapor-liquid interface
is in inverse proportion to the film thickness.

Figure 15 shows the comparison between the present data and existing boiling curve. Solid line shows the estimated heat flux from heat conduction analysis. The dash line shows the existing correlation heat flux, heat flux of nucleate boiling by Jons-Lottes[5], burn-out heat flux by Kutateladze[6], minimum heat flux of film boiling by Zuber[7] and heat flux of film boiling by Bromley[8].

It is shown from Fig. 15 that the estimated heat flux from the present experiment is much higher than the existing correlation.

4.2 PIV analysis

(1) Schematic and procedure of PIV analysis

In order to investigate the movement of the vapor-liquid interface, PIV technique was applied to the obtained visual data at the vapor liquid interface in the present experiment.

Figure 16 shows PIV analysis system in the present study and procedure to obtain the PIV analysis results. At first, digital video data was recorded with high-speed video camera of the maximum speed 40,500 fps. Secondly, time continuous two video data were analyzed with PIV software "VISIFLOW". As the result, velocity vector information is produced with the difference between two digital video data.

Figure 17 shows the schematic diagram of the PIV analysis algorithm. The algorithm is as follows:

1. Outline of vapor film taken for continuous time $t = t_1$ and $t = t_2$ are divided into 16 regions, respectively.
2. Each divided region of two pictures is moved a little in all direction to overlap between two pictures at time $t=t_1$ and $t=t_2$.
3. If two pictures are matched, the moving distance and angle are estimated. Then the velocity vector of the vapor-liquid interface movement is determined for one divided region.
4. These procedures are applied for all 16 regions. Finally, the velocity vector at the vapor-liquid interface movement are obtained for all regions.

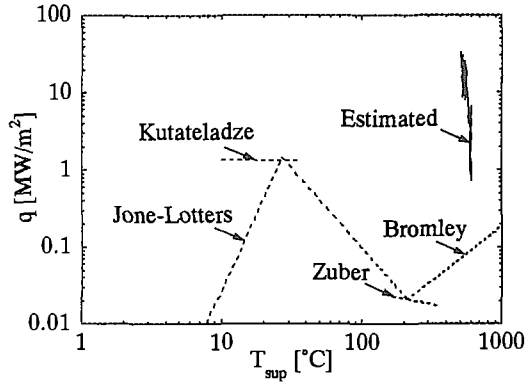

Fig. 15 Comparison with existing boiling curve

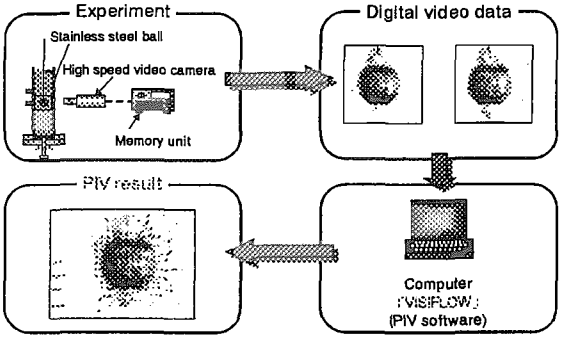

Fig. 16 PIV analysis system

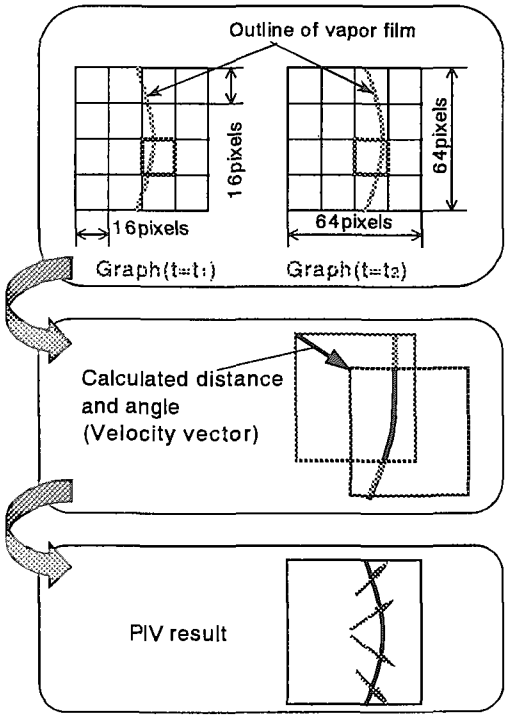

Fig. 17 Procedure of PIV analysis

(2) Results of the PIV analysis

One of the summaries of the analytical results of velocity field with PIV technique is shown in Fig. 18. Figure 18 shows the results in case that particle surface temperature is 1,000 °C and 600 °C, and subcooling are 10 °C and 60 °C. Vapor film was not established for the subcooling 60 °C at particle surface temperature 600 °C.

It is very difficult to estimate movement of the vapor-liquid interface by PIV technique, since the transient time of the phenomena is very short and view region is very narrow. Figure 18 shows the possibility that the vapor-liquid interface movement can be qualitatively followed by the present PIV technique.

4.3 Synthesis of heat conduction analysis and PIV analysis

Figure 19 shows the synthesis results of heat conduction analysis and the PIV analysis. All the data obtained in the present study are summarized in Fig. 19, that is, measured pressure and estimated vapor film thickness, measured particle surface temperature, saturation temperature estimated from the measured pressure and interfacial temperature estimated by the heat conduction analysis, visual information, and velocity vector of the vapor-liquid interface estimated with the PIV analysis.

The upper figure in Fig. 19 shows time transient of pressure and vapor film thickness. In this figure, vertical axes show pressure and vapor film thickness, and horizontal axis shows time in millisecond.

The middle figure in Fig. 19 shows time transient of interfacial temperature, saturation temperature and particle surface temperature. In this figure, vertical axes show interfacial temperature, saturation temperature and particle surface temperature, and horizontal axis shows time in millisecond. In both figures, the arrival time of pressure peak is taken as 0 ms. The lower figure in Fig. 19 shows picture taken from the visual observation, and the outline of vapor film and the velocity vector of the vapor-liquid interface movement. Symbols A to E correspond to figures above in Fig. 19.

Before the arrival of pressure wave, at time A, interfacial temperature was estimated higher than saturation temperature. And a clear and smooth vapor film was observed. Vapor film was not fluctuated.

When pressure pulse arrived, at time B, vapor film thickness reached its minimum value. Outlook of the vapor film changed white at time B. At this time, saturation temperature exceeded the interfacial temperature. Vapor film did not move in horizontal direction in PIV analysis.

The peak of pressure pulse was arrived at time C. The vapor film remained being white. Vapor film thickness was almost same as time B. Saturation temperature increased higher than the interfacial temperature. At this time, PIV result showed the vapor film moved toward the outside.

The pressure peak passed at time D. The boiling started on particle surface from visual information. At this time D, saturation temperature decreased across the vapor-liquid interfacial temperature. Vapor film moved toward particle surface in horizontal direction.

After the pressure pulse passed away, violent

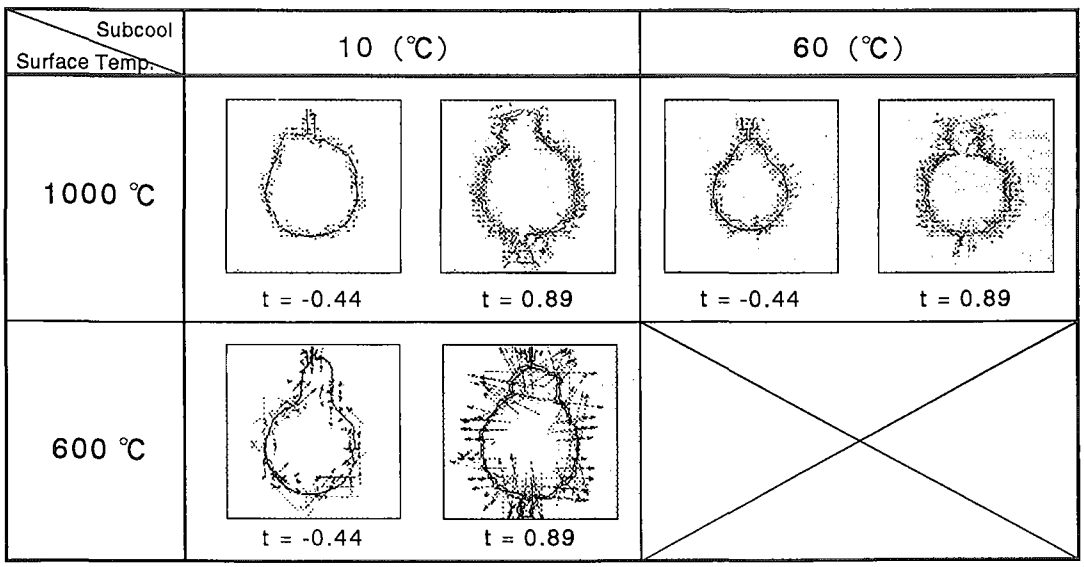

Fig. 18 Summaries of PIV analysis (unit: ms)

boiling was observed on particle surface at time E. The estimated vapor film thickness increased quickly. Correspondingly, estimated vapor-liquid interface with the PIV technique moved outward in horizontal direction. The estimated vapor-liquid interfacial temperature with heat conduction analysis became higher than the saturation temperature again.

5. Conclusions

1. The time transient of pressure, particle surface temperature, water temperature and visual information were simultaneously measured in the vapor film collapse experiment by external pressure pulse.
2. Film thickness is estimated by visual data processing technique with the pictures taken by the high-speed video camera.
3. Temperature and heat flux at the vapor-liquid interface were estimated by solving the heat conduction equation with the measured pressure, liquid temperature and vapor film thickness as boundary conditions.
4. Movement of the vapor-liquid interface were estimated with the PIV technique with the visual observation data.
5. Stable film boiling changed at the arrival time of pressure pulse. At the time, vapor-liquid interfacial temperature was estimated lower than the saturation temperature by the heat conduction analysis.
6. The estimated interfacial temperature exceeded again the saturation temperature after the pressure pulse passed away, and violent boiling started on the particle surface.

Nomenclature

C_p	: Specific heat at constant Pressure	$[J/kg\cdot K]$
D	: Steel particle diameter	$[m]$
g	: Gravitational acceleration	$[m/s^2]$
L	: Latent heat of vaporization	$[J/kg]$
p	: Pressure	$[N/m^2]$
Pr	: Prandtl number	$[-]$
q	: Heat flux	$[W/m^2]$
R	: Steel particle radius	$[m]$
r	: radial position	$[m]$
T	: Temperature	$[°C]$
t	: Time	$[s]$

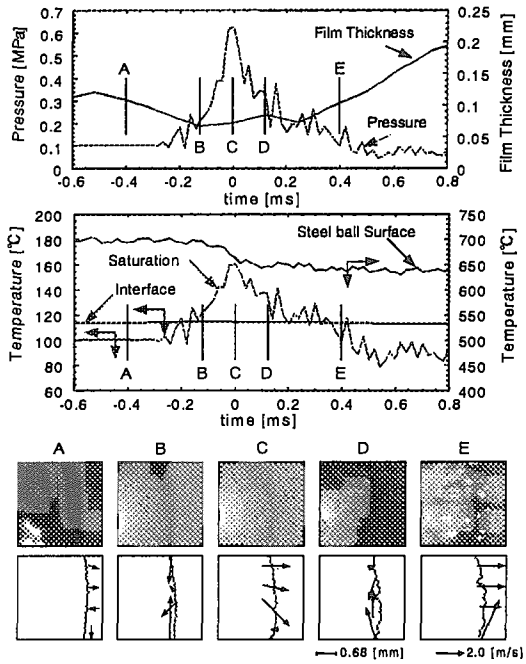

Fig. 19 Synthesis results from experiment and Analysis

Greeks

δ	: Vapor film thickness	$[m]$
κ	: Thermal diffusivity	$[m^2/s]$
ν	: Dynamic viscosity	$[m^2/s]$
σ	: Surface tension	$[N/m]$
λ	: Thermal conductivity	$[W/m\cdot K]$
ρ	: Density	$[kg/m^3]$

$\Delta\rho$: $= \rho_l - \rho_v$

Subscripts

l : Liquid
S : Steel particle
sat : Saturation
sup: Superheating
v : Vapor
w : Steel particle surface

Reference

[1] Board, S.J., Hall, R.W., Hall, R.S.:Nature, 254, 319 (1975)
[2] M. Yagi, Y. Abe, et. al., "Study of film collapse behavior during vapor explosion.", J. JSME, Ser. B, 65(636), pp.245-251(1999)
[3] Y. Abe and T. Kobayashi, "Study on vapor film collapse behavior on high temperature particle surface (1st report : Measurement of vapor film collapse pressure).", J. JSME, Ser. B, in printing.

[4] Y. Abe and D. Tochio, "Study on vapor film collapse behavior on high temperature particle surface (2nd report : Effect of subcooling on micro-mechanism).", J. JSME, Ser. B, in printing.
[5] W. H. Jens and P. A. Lottes, AEC Report, ANL-4627 (1951).
[6] S. S. Kutateladze, Zh. Tekh. Fiz., 20, p.1389 (1950).
[7] M. Zuber and M. Tribus, UCLA Report, 58-5 (1958).
[8] L. A. Bromley, Chem. Eng. Prog., 46-5, p.221, (1950).

Appendix

Theoretical heat flux in Fig. 15 is plotted with equations as follows:

(1) Mean heat flux of nucleate boiling by Jens-Lottes[5]

$$q_{Nu} = 2.56 \cdot T_{sup}^{4} \cdot \exp\left(\frac{p}{1.6954 \cdot 10^{6}}\right) \quad (A,1)$$

(2) Burn-out heat flux by Kutateladze[6]

$$q_{Bo} = 0.16 \cdot L\rho_{v} \cdot \left(\frac{\sigma g \Delta\rho}{\rho_{v}^{2}}\right)^{1/4} \quad (A,2)$$

(3) Minimum heat flux of film boiling by Zuber[7]

$$q_{Bo} = 0.157 \cdot L\rho_{v} \cdot \left(\frac{\sigma g \Delta\rho}{\rho_{l}^{2}}\right)^{1/4} \quad (A,3)$$

(4) Mean heat flux of film boiling by Bromley[8]

$$q_{Fi} = \frac{\lambda_{v}}{D} \cdot Nu_{Fb} \cdot T_{sup} \quad (A,4)$$

$$Nu_{Fb} = 0.62 \times \left\{\frac{g \cdot \Delta\rho \cdot D^{3}\, Pr_{v} \cdot \left(L + 0.5 \cdot C_{pv} \cdot T_{sup}\right)}{C_{pv}\rho_{v} \cdot T_{sup} \cdot \nu_{v}^{2}}\right\}^{1/4} \quad (A,5)$$

Cross points between (A,1) and (A,2), and (A,3) and (A,4) are calculated. Then, these points interpolated linearly to reproduce transition region.